AUTHOR QUERY FORM

Dear Author,

During the preparation of your manuscript for publication, the questions listed below have arisen. Please attend to these matters and return this form with your proof.

Many thanks for your assistance.

Query References	Query	Remarks
1	AUTHOR: Is author Mikihiro Fujiya the corresponding author for this article? Please confirm that this is correct. Also, please provide telephone and fax details and confirm that the email address is correct.	Yes, Mikihiro Fujiya is
2	AUTHOR: Please check and confirm if the heading levels are correct.	OK. No
3	AUTHOR: 'Membrane transport, which . . . waste from the cells'. This sentence has been reworded for clarity. Is the revision OK?	OK. No
4	AUTHOR: Is 'bacterial pathogenic bacterial components' here correct? Please change if incorrect.	We eliminate
5	AUTHOR: Is 'non-steroidal anti-inflammatory drug' the full form of NSAID? Please change if incorrect.	We added
6	AUTHOR: Please supply the full form of p38 MAPK.	We added the full
7	AUTHOR: Fujiya *et al*, Cell Host Microbe, 2007 has been changed to Fujiya *et al*, 2007 so that this citation matches the Reference List. Please confirm that this is correct.	OK. No
8	AUTHOR: Okamoto *et al*, 2012 has not been included in the Reference List. Please supply full publication details.	We added
9	AUTHOR: Segawa *et al*, PLoS ONE, 2011 has been changed to Segawa *et al.*, 2011 so that this citation matches the Reference List. Please confirm that this is correct.	OK. No
10	AUTHOR: Vavricha SR, Gastroenterology, 2004 has been changed to Vavricka *et al.*, 2004 so that this citation matches the Reference List. Please confirm that this is correct.	Ok. No
11	AUTHOR: Veiga E, 2005 has not been included in the Reference List. Please supply full publication details.	We added
12	AUTHOR: Fujiya M, Cell Host & Microbe, 2007 has been changed to Fujiya *et al.*, 2007 so that this citation matches the Reference List. Please confirm that this is correct.	OK. No
13	AUTHOR: Okamoto K, 2012 has not been included in the Reference List. Please supply full publication details.	We added
14	AUTHOR: Ng J, Gastroenterology, 2010 has been changed to Ng *et al.*, 2010 so that this citation matches the Reference List. Please confirm that this is correct.	OK. No
15	AUTHOR: Papatheodorou P, PLoS ONE, 2010 has been changed to Papatheodorou *et al.*, 2010 so that this citation matches the Reference List. Please confirm that this is correct.	OK. No

Query References	Query	Remarks
16	AUTHOR: Uemura T, Am J Physiol Gastrointest Liver Physiol, 2010 has been changed to Uemura *et al.*, 2010 so that this citation matches the Reference List. Please confirm that this is correct.	OK. No
17	AUTHOR: Matumoto M, PLoS ONE, 2011 has been changed to Matumoto *et al.*, 2011 so that this citation matches the Reference List. Please confirm that this is correct.	OK. No
18	AUTHOR: Segawa S, PLoS ONE, 2011 has been changed to Segawa *et al.*, 2011 so that this citation matches the Reference List. Please confirm that this is correct.	OK. No
19	AUTHOR: Konishi H, Digestive Disease Week, 2013 has been changed to Konishi *et al.*, 2013 so that this citation matches the Reference List. Please confirm that this is correct.	OK. No
20	AUTHOR: As per journal style, abbreviations for genes should be set in italic, whereas abbreviations for gene products (enzymes/proteins) should be set in roman (upright). Please check throughout the article and ensure that this is followed. Also, no need to spell out genes and gene product abbreviations.	We changed
21	AUTHOR: If SLC15 is an abbreviation, please supply its full form.	We
22	AUTHOR: Please supply the full form of Tri-DAP.	We
23	AUTHOR: Please supply the full form of ERK1/2.	We
24	AUTHOR: Are 'Crohn's disease' and 'ulcerative colitis' the full forms of CD and UC respectively? Please change if incorrect.	OK. No
25	AUTHOR: Fujiya *et al*, Inflamm Bowel Dis. 2011 has been changed to Fujiya *et al.*, 2011 so that this citation matches the Reference List. Please confirm that this is correct.	OK. No
26	AUTHOR: Is 'wild-type' the full form of WT? Please change if incorrect.	OK. No
27	AUTHOR: 'Jr' has been added in reference citation 'Chidlow *et al.* 2009' to conform journal style. Please confirm that this is correct.	OK. No
28	AUTHOR: Matumoto *et al*, 2011 has been changed to Matsumoto *et al*, 2011 so that this citation matches the Reference List. Please confirm that this is correct.	OK. No
29	AUTHOR: If there are fewer than 8 authors, please supply all of their names. If there are 8 or more authors, please supply the first 6 authors' names then *et al.* throughout the ref list.	We added

Oncogene (2014) **33,** 4847–4856

www.nature.com/onc

ORIGINAL ARTICLE

microRNA-18a induces apoptosis in colon cancer cells via the autophagolysosomal degradation of oncogenic heterogeneous nuclear ribonucleoprotein A1

M Fujiya[1], H Konishi[1], MK Mohamed Kamel[1], N Ueno, Y Inaba, K Moriichi, H Tanabe, K Ikuta, T Ohtake and Y Kohgo

It is well known that microRNAs (miRs) are abnormally expressed in various cancers and target the messenger RNAs (mRNAs) of cancer-associated genes. While (miRs) are abnormally expressed in various cancers, whether miRs directly target oncogenic proteins is unknown. The present study investigated the inhibitory effects of miR-18a on colon cancer progression, which was considered to be mediated through its direct binding and degradation of heterogeneous nuclear ribonucleoprotein A1 (hnRNP A1). An MTT assay and xenograft model demonstrated that the transfection of miR-18a induced apoptosis in SW620 cells. A binding assay revealed direct binding between miR-18a and hnRNP A1 in the cytoplasm of SW620 cells, which inhibited the oncogenic functions of hnRNP A1. A competitor RNA, which included the complementary sequence of the region of the miR-18a-hnRNP A1 binding site, repressed the effects of miR-18a on the induction of cancer cell apoptosis. *In vitro* single and *in vivo* double isotope assays demonstrated that miR-18a induced the degradation of hnRNP A1. An immunocytochemical study of hnRNP A1 and LC3-II and the inhibition of autophagy by 3-methyladenine and ATG7, p62 and BAG3 siRNA showed that miR-18a and hnRNP A1 formed a complex that was degraded through the autophagolysosomal pathway. This is the first report showing a novel function of a miR in the autophagolysosomal degradation of an oncogenic protein resulting from the creation of a complex consisting of the miR and a RNA-binding protein, which suppressed cancer progression.

Oncogene (2014) **33,** 4847–4856; doi:10.1038/onc.2013.429; published online 28 October 2013

Keywords: microRNAs; heterogeneous nuclear ribonucleoproteins; colon cancer; apoptosis; autophagy; ubiquitin

INTRODUCTION

Colon cancer is one of the most common causes of cancer-related death in both eastern and western countries. The etiology of colon cancer is associated with genetic and epigenetic abnormalities, including mutations of the *k-ras*, *p53* and *Apc* genes, as well as hypermethylation of the *p16* and *DNA mismatch repair* genes.[1–5] Conversely, recent studies have proposed that, in addition to these DNA abnormalities, the abnormal expression of non-coding RNAs, which account for 97% of all non-ribosomal RNAs in eukaryotes, is also involved in the pathogenesis of tumors.[6] Non-coding RNAs do not code for amino acid sequences, but instead post-transcriptionally regulate the expression of proteins.[7] MicroRNA (miR) are a type of Non-coding RNAs, are short (20–23-nucleotide), endogenous and single-stranded RNA sequences found in almost all eukaryotic cells.[8,9] miRs bind to messenger RNAs (mRNAs) based on their sequence complementarity and regulate the translation of target mRNAs.[10–14] Some miRs, including miR-15 and -16, let-7 and the miR-17-92 cluster,[15–18] are abnormally expressed in tumor cells in various organs, including the colon, and function as suppressors or enhancers of tumor progression. It is thought that miRs regulate the translation of the mRNAs of tumor-related proteins by binding to the mRNAs, as exemplified by the downregulation of MYC by let-7a in lymphoma cells[19] and let-7a in hepatocellular carcinoma and breast cancer cells.[20,21] The targets of each miR appear to be dependent on the organ and histological type of cancer.

miR-18a is highly expressed in several cancer cell types and is thought to be a tumor suppressor.[20,22] The targets of miR-18a have been reported to be the mRNAs of the estrogen receptors in hepatocellular carcinoma[20] and dicer in bladder cancer.[22] However, the target of miR-18a in colon cancer has not been identified, although miR-18a is highly expressed in colon cancer cells.[23]

Conversely, a recent investigation proposed that miR may regulate the protein function without modifying the translation of the mRNA.[24] The authors of that study showed that miR-328 directly binds to heterogeneous nuclear ribonucleoprotein (hnRNP) E2, an RNA binding protein, and inhibits the function of hnRNP E2, leading to the destabilization of the mRNA for CCAAT/enhancer-binding protein alpha in leukemic blasts. This suggests that miRs can inhibit the function of target proteins, particularly RNA-binding proteins (such as those of the hnRNP family), by directly binding to the proteins without influencing the translation of the mRNA. However, the role of the direct binding between proteins and miRs on the physiological function of cells is unclear. We hypothesized that some miRs inhibit the progression of cancer cells by directly binding to RNA-binding proteins, such as hnRNPs, which possess oncogenic properties, and inducing the degradation of these proteins.

This study demonstrates that miR-18a induces the apoptosis of colon cancer cells by directly binding to oncogenic hnRNP A1,which has a binding site for miR-18a[25,26] and leads to the evasion of cancer cell apoptosis, followed by the autophagolysosomal degradation of the protein.

Division of Gastroenterology and Hematology/Oncology, Department of Medicine, Asahikawa Medical College, Asahikawa, Japan. Correspondence: Dr M Fujiya, Division of Gastroenterology and Hematology/Oncology, Department of Medicine, Asahikawa Medical College, 2-1 Midorigaoka-higashi, Asahikawa, Hokkaido 078-8510, Japan.
E-mail: fjym@asahikawa-med.ac.jp
[1]These authors contributed equally to this work.
Received 24 January 2013; revised 12 August 2013; accepted 26 August 2013; published online 28 October 2013

RESULTS

Overexpression of miR-18a induces the apoptosis of colon cancer cells

A real-time PCR analysis showed that miR-18a is endogenously expressed in human colon cancer tissues (Supplementary Figure 1A) as well as all colon cancer cell lines examined, including Caco2/bbe, HT29, HCT-116, SKCO-1, SW480 and -620 cells (Supplementary Figure 1B). Double-stranded miR-18a was transfected into colon cancer cell lines to examine the effects of the overexpression of miR-18a on colon cancer progression. A significant augmentation of the miR-18a expression was detected in all cell lines, particularly in the SW620 and HCT116 cells (Supplementary Figure 2), while miR-18a*, the complimentary strand of miR-18a, did not increase the level of apoptosis after its transfection into SW620 cells (Supplementary Figure 3). To examine the relationship between cell viability and miR-18a expression, the MTT assay was performed in SW620 and HCT116 cells with up- or downregulated expression of miR-18a. The MTT assay showed that, while there were no changes in the cell density between the miR-18a overexpressing cells and the control cells within 48 h, the cell density was significantly decreased in the miR-18a-overexpressing cells in comparison to the levels observed in the control 72 and 96 h after transfection into SW620 cells. Conversely, in miR-18a-knockdown cells, the cell viability was not changed in comparison to that of the control at any of the time points in SW620 cells (Figure 1a, (Supplementary Figure 4). The cell viability was significantly decreased in miR-18a-overexpressing HCT116 cells and significantly increased in miR-18a-knockdown HCT116 cells (Figure 1b).

To assess the *in vivo* impact of the miR, a suspension of 1×10^6 SW620 cells was injected into the backs of nude mice to generate a xenograft model in order to confirm the suppressive effects of miR-18a overexpression on colon cancer progression. Double-stranded miR-18a or control RNA inserted in a Sendai virus envelope was injected every day into the tumors beginning the day after implantation of the cells, and the tumor sizes were measured. Figure 1c shows that the increase in the size of the tumors in the miR-18a-injected group was almost completely suppressed (1.1-fold), while the tumors in the control group increased in size by 1.6-fold. Moreover, SW620 cells that stably overexpressed miR-18a or a control vector were injected into nude mice using the same methods. The tumor size increased rapidly in the mice injected with SW620 cells treated with the control vector, but not in the cells stably overexpressing miR-18a (Figure 1d).

Immunocytochemical staining showed the Ki-67 expression to not be significantly different between the miR-18a-overexpressing cells and control cells (Supplementary Figure 5). TUNEL staining showed that there was a significant increase in the number of TUNEL-positive miR-18a overexpressing cells compared to the control and miR-18a knockdown cells (Figure 1e).

A western blotting analysis also showed that the expression levels of cleaved caspases −3, −9 and PARP were significantly increased in the miR-18a-overexpressing cells in comparison to the level observed in the control cells (Figure 1f). The cell population in each phase of the cell cycle was examined using flow cytometry. A telomere length assay revealed that the telomere length was shorter in the miR-18a-overexpressing cells than in the control cells (Supplementary Figure 6). Therefore, the overexpression of miR-18a inhibited colon cancer progression by inducing the apoptosis of the cancer cells.

miR-18a induces cancer cell apoptosis by suppressing hnRNP A1

It has been hypothesized that miR-18a targets oncogenic proteins, particularly members of the hnRNP family, a group of RNA-binding proteins.[24] hnRNP A1 possesses binding sites for miR-18a;[25,26] therefore, hnRNP A1 was the focus of the subsequent experiments. Real-time PCR showed that the mRNA for hnRNP A1 is highly expressed in colon cancer tissues and cell lines[27] (Supplementary Figures 7A–C). To determine whether the effects of miR-18a on the suppression of cancer cell progression were dependent on the expression of hnRNP A1, SW620 cells were transfected with miR-18a with or without hnRNP A1 siRNA. Targeting hnRNP A1 with siRNA inhibited cancer cell progression. Notably, the inhibitory effect induced by miR-18a was repressed in the cells transfected with the hnRNP A1 siRNA (Figure 2a). A competitor RNA with a complimentary sequence to the binding site of miR-18a to hnRNP A1 negated the cancer cell apoptosis induced by the overexpression of miR-18a (Figure 2b).

It is known that hnRNP A1 stabilizes the mRNAs of cyclin D1 and CTGF, while increasing the expression levels of these molecules, which are associated with the evasion of apoptosis.[28,29] The expression levels of cyclin D1 and CTGF were therefore examined to determine whether the overexpression of miR-18a inhibits the function of hnRNP A1. Figure 2c shows that the cyclin D1 and CTGF expression levels were significantly decreased in the SW620 cells overexpressing miR-18a. The competitor RNA repressed the downregulation of cyclin D1 and CTGF (Figures 2d and e). Conversely, the overexpression of miR-18a did not change the translation of the mRNAs encoding cell growth- and apoptosis-associated molecules, which were selected based on previous reports and were estimated targets of mRNAs in an analysis of microRNA sequences using a software program (**Targetscan, http://www.targetscan.org/vert_50/**)(Supplementary Figure 8). These findings indicate that the miR-18a-induced apoptosis of cancer cells is mediated by the creation of a complex between miR-18a and hnRNP A1.

miR-18a binds to hnRNP A1 in the cytoplasm of colon cancer cells

A binding assay demonstrated the ratio of miR-18a bound to hnRNP A1 in cell lines, including HEK 293, Caco2/bbe, HT29, HCT116, SKCO-1, SW480 and -620 cells. The HEK 293 cells were selected as non-cancer cells. The ratio of binding between miR-18a and hnRNP A1 varied in these cell lines. Approximately 8% and 30% of all miR-18a were bound to hnRNP A1 in the SW620 and HCT116 cells, respectively, while 58% of the endogenous miR-18a was bound to hnRNP A1 in the HEK cells. The binding between miR-18a and hnRNP A1 was increased 5.5-fold and 7-fold in the miR-18a-overexpressing SW620 and HCT116 cells, respectively (Figure 3a).

FITC-labeled miR-18a was transfected into the SW620 cells to assess the interaction between this protein and hnRPN A1. A western blotting analysis with immunoprecipitation and a binding assay showed that FITC-labeled miR-18a bound to hnRNP A1 was detected primarily in the cytoplasm of the SW620 cells (Figures 3b and c and Supplementary Figure 9). These findings suggest that miR-18a directly binds to hnRNP A1 in the cytoplasm of colon cancer cells.

miR-18a induces the degradation of hnRNP A1

The hnRNP A1 expression was assessed by a western blotting analysis at 3, 6, 24, 48, 72 and 96 h after transfection with miR-18a to determine whether the hnRNP A1 expression was changed by the binding to miR-18a. The hnRNP A1 expression was significantly decreased at 72 and 96 h after miR-18a transfection, while no changes in the hnRNP A1 expression were observed within 48 h (Figure 4a). Notably, the decreased expression of the hnRNP A1 protein induced by the overexpression of miR-18a was repressed by treatment with the competitor of miR-18a at 72 h, suggesting that the decreased expression of hnRNP A1 is mediated by the creation of a complex between miR18a and hnRNP A1 (Figure 4b). The mRNA level of hnRNP A1 was not decreased at 3, 8, 24, 48, 72 or 96 h (Figure 4c). Similarly, a xenograft model demonstrated that the expression of hnRNP A1 proteins, but not mRNA, was significantly lower in the tumors

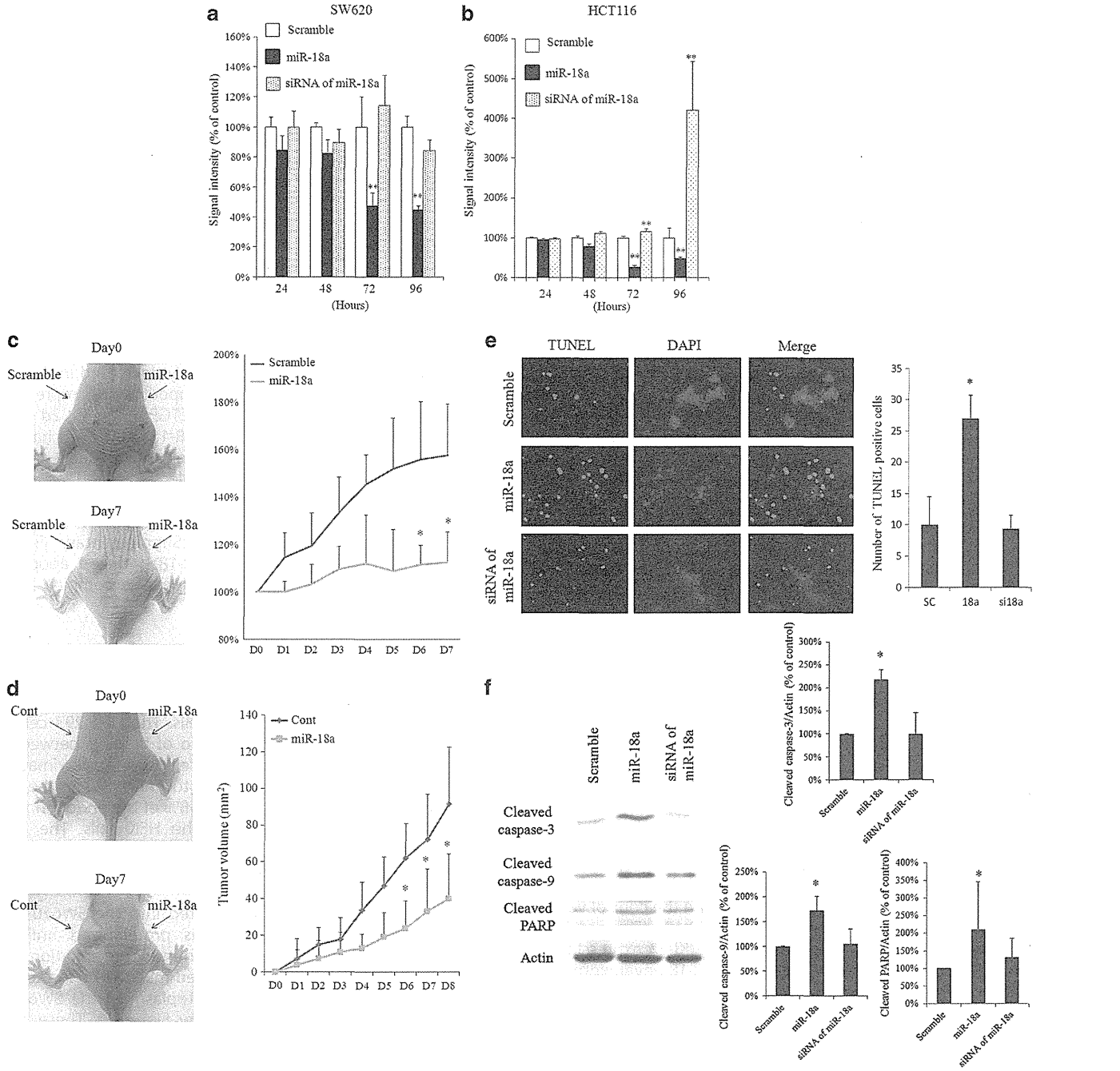

Figure 1. The overexpression of miR-18a induces the apoptosis of colon cancer cells. An MTT assay revealed that the number of live SW620 cells was significantly lower in the miR-18a overexpression group than in the control group at 72 and 96 h after transfection ($n = 5$) (**a**). An MTT assay showed that the viability of HCT116 cells was significantly lower in the miR-18a overexpression group and higher in the miR-18a siRNA-treated group than in the control group at 72 and 96 h after transfection ($n = 5$) (**b**). The xenograft model showed that the enlargement of the tumors in the miR-18a-injected group was almost completely suppressed (1.1-fold), while the tumors in the control group were enlarged as much as 1.6-fold ($n = 6$) (**c**). miR-18a stably-overexpressing and control SW620 cells were used to generate another xenograft model. The model showed that the tumor size was significantly smaller in the xenografts from SW620 cells stably overexpressing miR-18a than in the tumors generated from control cells (**d**). TUNEL staining showed the level of apoptosis to increase in the SW620 cells transfected with miR-18a in comparison to that in the cells transfected with scramble RNA (**e**). A western blotting showed analysis that the cleaved caspase-3, -9 and PARP expression levels were significantly higher in the SW620 cells transfected with double-stranded miR-18a ($n = 3$) (**f**). $^{*}P < 0.05$, $^{**}P < 0.01$.

injected with double-stranded miR-18a than in those injected with control RNA (Figure 4d). Therefore, miR-18a post-transcriptionally decreases the protein expression of hnRNP A1 by binding to hnRNP A1.

Next, the degradation rate of hnRNP A1 was assessed using single and double isotope studies to determine whether miR-18a induces its degradation. A single isotope study showed that the ^{3}H activity was significantly lower in SW620 cells transfected with double-stranded miR-18a than in control cells at 72 to 96 h after transfection (Supplementary Figure 10). An *in vivo* double isotope study confirmed that the $^{3}H/^{14}C$ ratio was significantly lower in mice transfected with double-stranded miR-18a than in those

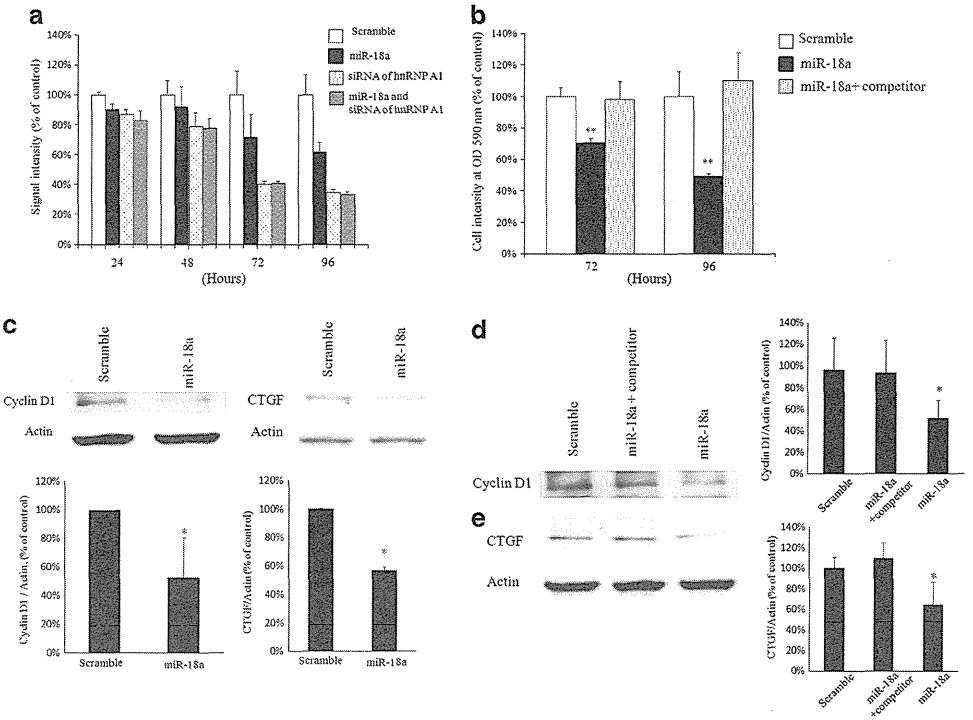

Figure 2. miR-18a induces cancer cell apoptosis by binding to hnRNP A1 and suppressing its functions. A MTT assay revealed that the overexpression of miR-18a inhibited cancer cell progression, and a siRNA targeting hnRNP A1 also inhibited cancer cell progression. The inhibitory effect of miR-18a on cancer cell progression was negated in the cells transfected with the hnRNP A1 siRNA ($n=5$) (**a**). A competitor RNA with a complimentary sequence to the binding site of miR-18a to hnRNP A1 repressed the apoptosis induced by the overexpression of miR-18a (**b**). The expression levels of cyclin D1 ($n=4$) and CTGF ($n=3$), which were upregulated by hnRNP A1, were significantly decreased in SW620 cells overexpressing miR-18a. The upper figure shows western blots and the lower one shows the results of the densitometry analysis (**c**). The competitor RNA negated the downregulation of cyclin D1 ($n=4$) (**d**) and CTGF ($n=4$) induced by the overexpression of miR-18a (**e**). $^{*}P<0.05$, $^{**}P<0.01$.

injected with control cells, suggesting that miR-18a induces the degradation of the hnRNP A1 protein (Figure 4e).

The degradation of hnRNP A1 by miR-18a is mediated by autophagy

The ubiquitination of hnRNP A1 bound to miR-18a was evaluated using a Western blotting analysis to examine the mechanisms underlying the degradation of hnRNP A1 by miR-18a. The ubiquitinated hnRNP A1 band was significantly increased in the miR-18a-overexpressing cells at 72 and 96 h in comparison with that observed in the control cells, while no changes were observed in the higher molecular bands in any group (Figure 5a). This suggests that the ubiquitination of hnRNP A1 is augmented by miR-18a overexpression, and that this leads to the subsequent proteasomal or lysosomal degradation of the protein. We then confirmed that 3-methyladenine, an inhibitor of autophagy, negated the effects of miR-18a overexpression on the hnRNP A1 expression (Figure 5b). In contrast, MG132, an inhibitor of the proteasome, did not affect the expression of hnRNP A1 (Supplementary Figure 11).

An immunocytochemical study demonstrated the coexpression of hnRNP A1 and LC3-II, a component of autophagosomes (Figure 5c). A western blotting analysis with immunoprecipitation showed that FITC-labeled miR-18a formed a complex with LC3-II and hnRNP A1 (Figure 5d). A siRNA targeting ATG7, which is also a mediator of the creation of autophagosomes, repressed the downregulation of hnRNP A1 induced by miR-18a (Figure 5e). Treatment of cells with siRNAs against both p62, a well-known molecule that selectively brings ubiquitinated proteins to autophagosomes,[30] and BAG3, which is required to process autophagolysosomal degradation,[31] also negated the decrease in the hnRNP A1 expression induced by miR-18a (Figure 5f, Supplementary Figure 12).

To examine whether normal cells possess a mechanism leading to the autophagosomal degradation of hnRNP A1 via binding with miR-18a, we performed a binding assay and a Western blotting analysis in HEK293 cells. The binding assay showed that 58% of the endogenous miR-18a bound to hnRNP A1 (Figure 3a). The western blotting analysis showed that miR-18a downregulates hnRNP A1, and this function of miR-18a is diminished by the knockdown of autophagy-related genes, such as ATG7 and p62, in HEK293 cells (Supplementary Figure 13). These results indicate that miR-18a-bound hnRNP A1 is selectively degraded by the autophagosomal pathway in cancer cells, as well as in normal cells.

DISCUSSION

The present study demonstrated that miR-18a inhibits colon cancer progression through the induction of cancer cell apoptosis. The antitumor effect of miR-18a was repressed by the treatment of cells with a competitor for the miR-18a-hnRNP A1 interaction and by the inhibition of the autophagolysosomal pathway with a specific inhibitor or with siRNAs targeting ATG7, p62 and BAG3, thus indicating that the effect of miR-18a is due to its interaction with oncogenic hnRNP A1, and the subsequent induction of the autophagolysosomal degradation of the protein. These data suggest that miRs can exert inhibitory effects on cancer progression by inducing the degradation of oncogenic proteins (Figure 6).

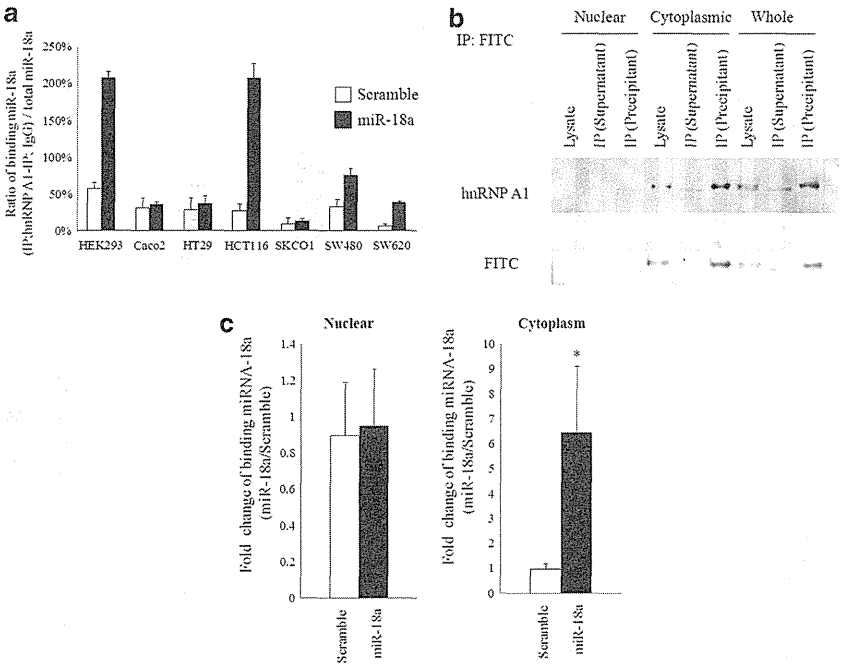

Figure 3. miR-18a binds to hnRNP A1 in the cytoplasm of colon cancer cells. The cells and tissues were lysed and immunoprecipitated using IgG and hnRNP A1 antibodies. RNA was extracted and the miR-18a expression was measured using real-time PCR (a binding assay). The assay showed that the ratio of binding between miR-18a and hnRNP A1 varied by cell line. Approximately 8% and 30% of miR-18a molecules were bound to hnRNP A1 in the SW620 and HCT116 cells, respectively, while 58% of miR-18a was bound to hnRNP A1 in HEK 293 cells (**a**). The proteins in the nucleus and cytoplasm of SW620 cells transfected with FITC-labeled miR-18a were separately extracted and immunoprecipitated with anti-FITC antibodies. The expression of hnRNP A1 was examined by a western blot analysis. The upper blot was detected by a western blot analysis with immunoprecipitation by anti-hnRNP antibodies. The lower blot was detected with immunoprecipitation by anti-FITC antibodies. The hnRNP A1 bound to miR-18a was primarily expressed in the cytoplasm of SW620 cells (**b**). A binding assay showed that the FITC-labeled miR-18a bound to hnRNP A1 was primarily detected in the cytoplasm of SW620 cells (**c**). ($n = 3$) $^*P < 0.05$.

miRs generally function by controlling the translation of mRNAs in cancer cells. For example, let-7a inhibits the translation of MYC mRNA in lymphoma cells.[19] miR-107, -22, -143, -34a and -21 target the mRNAs of HIF-1,[32] p21,[33] metastasis-associated in colon cancer-1,[34] fos-related antigen 1,[35] and transforming growth factor beta receptor 2[36] in colon cancer cells, respectively. The mRNA of estrogen receptors is targeted by miR-18a in hepatocellular carcinoma cells,[20] breast cancer cells[21] and dicers in bladder cancer cells;[22] however, the target of miR-18a in colon cancer had not been identified, although miR-18a is highly expressed in colon cancer cells.[23] Recently, Eiring *et al.*[24] proposed the possibility that miRs directly bind to target proteins and inhibit the protein functions and concluded that miRs can target not only mRNAs but also proteins. However, the role of binding between miRs and hnRNPs in cancer progression and the fate of the miR-hnRNP A1 complex have not yet been clarified. The present study demonstrated, for the first time, that the binding between miR-18a and hnRNP A1 is a trigger for the ubiquitination and degradation of oncogenic hnRNP A1 via the autophagolysosomal pathway. Therefore, the overexpression of miR-18a is thought to continuously, not temporally, inhibit the oncogenic function of hnRNP A1. No therapeutic strategies for treating colon cancers by targeting hnRNPs have thus far been established. However, miR-18a transfection is a feasible option for treating colon cancers, and possibly other types of cancers in which hnRNP A1 is upregulated.

The present study showed that transfected miR-18a is bound to hnRNP A1 in the cytoplasm of colon cancer cells. Most hnRNP A1 is expressed in the nucleus in normal epithelia, binds to pri-miR-18a and contributes to the maturation of miR-18a.[25] Mature miR-18a is then transported from the nucleus to the cytoplasm, where it controls the translation of mRNAs. The present study suggests that when the hnRNP A1 expression is increased in normal cells, the maturation of miR-18a is promoted in the nucleus, and the increased mature miR-18a is thereafter transported to the cytoplasm, where it degrades the overexpressed hnRNP A1. This appears to be a feedback system between miRs and hnRNPs. Conversely, this feedback system is thought to be impaired in cancer cells because hnRNPs, including hnRNP A1, -I and K, are highly expressed in the cytoplasm of colon cancer cells, particularly in metastatic lymph nodes. The excess expression of cytoplasmic hnRNPs appears to promote with the malignant behavior of colon cancer.[37] Accordingly, mature miR-18a is thought to create a complex with excessively-expressed hnRNP A1 in the cytoplasm and inhibits its function by inducing autophagolysosomal degradation. The present study also showed that, while the expression levels of both miR-18a and hnRNP A1 are increased in colon cancer cells, the transfection of mature miR-18a still inhibits cancer progression by inducing apoptosis both *in vitro* and *in vivo*. Our binding assay showed that, in colon cancer cells (SW620 cells), only 8% of the miR-18a molecules are bound to hnRNP A1, whereas 58% of endogenous miR-18a in HEK 293 cells was present in a complex with hnRNP A1, suggesting that a large amount of free hnRNP A1 is present in the cytoplasm and exerts its oncogenic functions in cancer cells by binding to target mRNAs. Transfection of miR-18a increased the miR-18a-hnRNP A1 complex 6-fold, thereby inhibiting the oncogenic functions of hnRNP A1.

The present study proposes that miR-18a induces the degradation of hnRNP A1 through the autophagolysosomal pathway. It has recently been shown that miR-18a upregulated the autophagy and gene expression of ataxia telangiectasia mutated, which

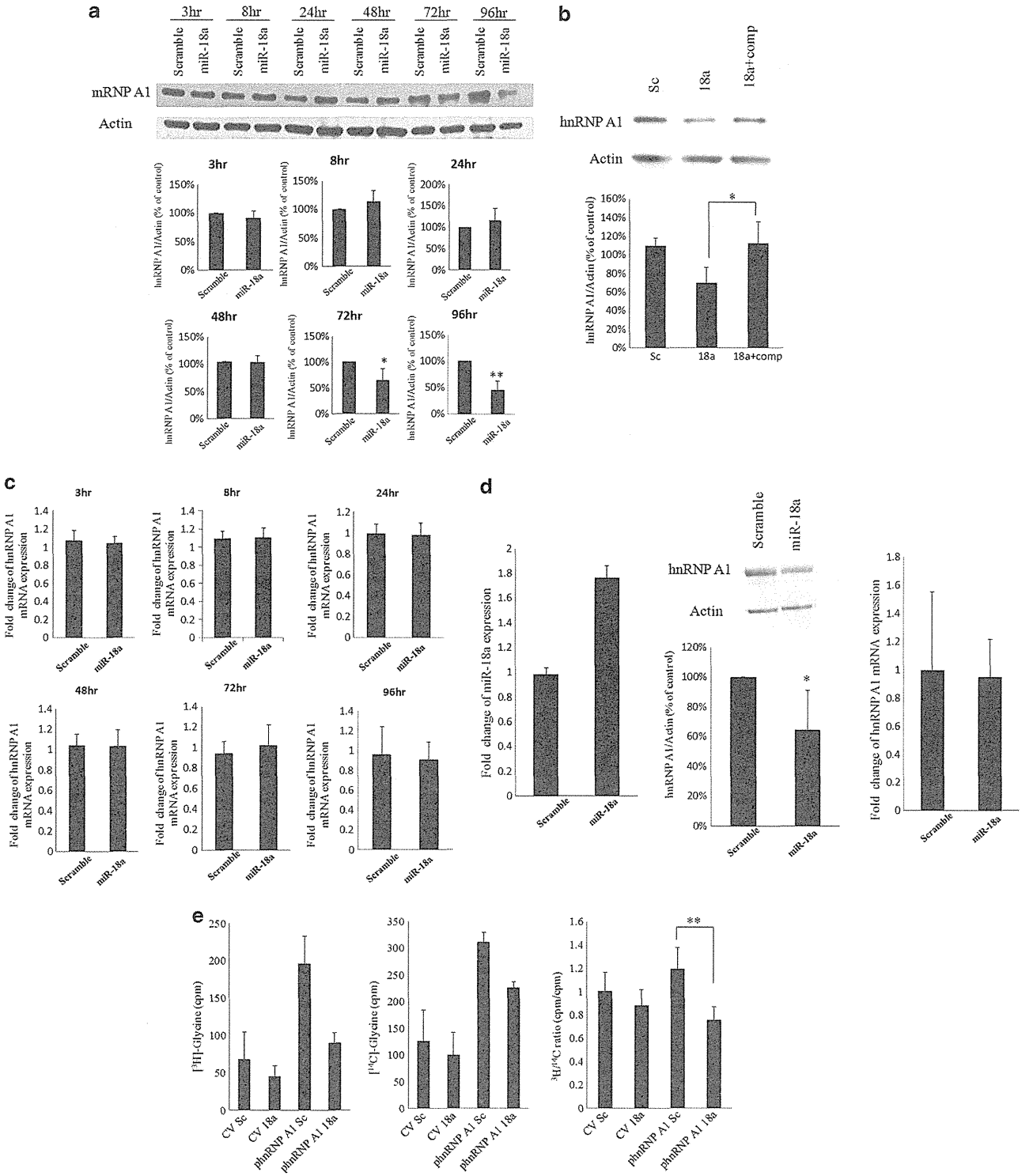

Figure 4. miR-18a induces the degradation of hnRNP A1. The expression of hnRNP A1 was assessed by a western blotting analysis at 24, 48, 72 and 96 h after transfection of the cells with miR-18a. The hnRNP A1 expression was significantly decreased at 72 and 96 h after miR-18a transfection ($n=3$) (**a**). The decreased expression of hnRNP A1 proteins induced by the overexpression of miR-18a was negated by treatment with the competitor of miR-18a ($n=3$) (**b**). The hnRNP A1 mRNA level did not decrease at 3, 8, 24, 48, 72 or 96 h after transfection with miR-18a ($n=3$) (**c**). A xenograft model showed that the expression of miR-18a was increased (left) and the expression of hnRNP A1 protein was decreased (center) in the tumors injected with double-stranded miR-18a, in comparison to that observed in the tumors injected with control RNA, while the hnRNP A1 mRNA level was not significantly different in these groups (right) ($n=3$) (**d**). The mice were injected with 100 μCi of [^{3}H]-glycine 3 h after transfection of the expression vector for hnRNP A1 and/or double-stranded miR-18a. The mice were again injected with an expression vector for hnRNP A1 72 h later. The mice were injected with 12.5 μCi of [14C]-glycine 3 h later and then were killed after an additional 3 h. Protein samples obtained from the intestines were immunoprecipitated with hnRNP A1 antibodies, and the radioactivity was measured (a double isotope study). This assay showed that the $^3H/^{14}C$ ratio was significantly lower in the mice transfected with double-stranded miR-18a than in those injected with the control cells ($n=3$) (**e**). $^*P<0.05$, $^{**}P<0.01$.

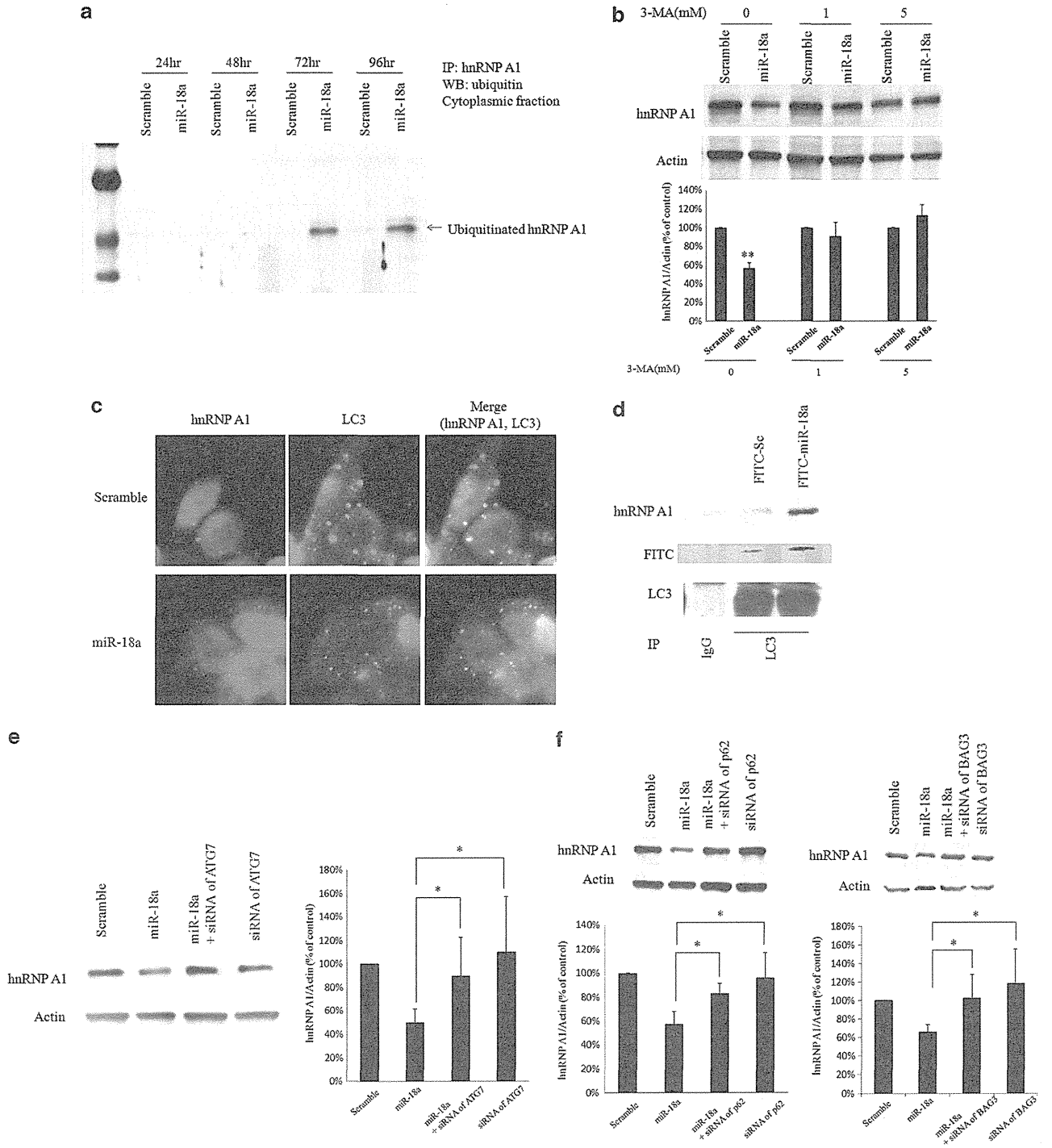

Figure 5. Autophagy mediates the degradation of hnRNP A1 by miR-18a in colon cancer cells. A western blotting analysis revealed that ubiquitinated hnRNP A1 band was significantly increased in miR-18a-overexpressing cells in comparison to that observed in the control cells at 72 and 96 h, while there were no significant differences in the intensities of the higher molecular bands between the groups ($n=3$) (**a**). 3-methyladenine, an inhibitor of autophagy, repressed the inhibitory effects of miR-18a overexpression on the expression of hnRNP A1 ($n=3$) (**b**). Immunocytochemistry demonstrated the coexpression of hnRNP A1 and LC3-II, a component of autophagosomes ($n=3$) (**c**). A western blotting analysis using immunoprecipitation with anti-FITC antibodies in SW620 cells transfected with FITC-labeled miR-18a showed that miR-18a formed a complex with hnRNP A1 and LC3-II, an essential component of the autophagy process ($n=6$) (**d**). Treatment with a siRNA targeting ATG7, an essential mediator of the creation of autophagosomes, repressed the effects of miR-18a on the downregulation of hnRNP A1 ($n=3$) (**e**). The treatment with a siRNA targeting p62, which selectively brings ubiquitinated proteins to autophagosomes, also repressed the decrease in the hnRNP A1 expression induced by miR-18a ($n=3$) (left). This also occurred following treatment with a siRNA targeting BAG3, which is required for the process of autophagolysosomal degradation ($n=3$) (right) (**f**). $^{*}P<0.05$, $^{**}P<0.01$.

enhanced the autophagy process.[38] Taken together, these findings suggest that miR-18a induces the degradation of oncogenic hnRNP A1 by forming a complex with the protein, as well as by enhancing the autophagy pathway itself. miR-18a is therefore considered to be a multifunctional molecule which regulates both gene expression and protein degradation.

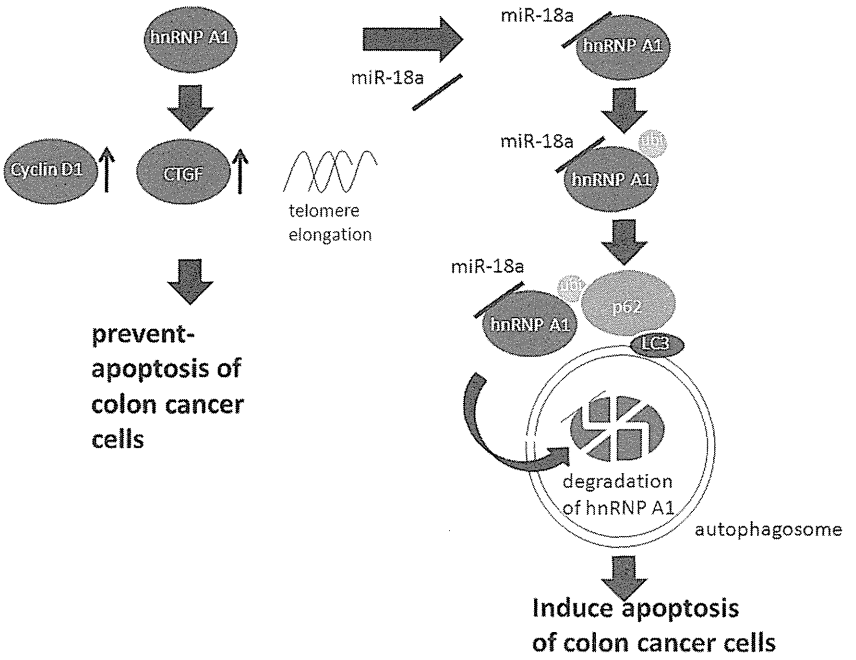

Figure 6. A scheme of the miR-18a-mediated pathway that induces the apoptosis of colon cancer cells. miR-18a inhibits colon cancer progression by inducing cancer cell apoptosis by binding to oncogenic hnRNP A1 and inducing the autophagolysosomal degradation of the protein.

In summary, the current study proposed a novel function of miR-18a in the inhibition of colon cancer progression via the binding and downregulation of oncogenic hnRNP A1 in the cytoplasm. This function is considered to be reproducible for other miRs, thus providing new insights into the eventual development of new therapeutic strategies to treat various malignancies in which hnRNPs are associated with tumor progression.

MATERIALS AND METHODS

Human intestinal epithelia

Biopsy specimens of normal mucosa were obtained from the colons of patients with colon cancer during colonoscopy. Written informed consent was obtained from all patients, and the ethics committee of Asahikawa Medical University gave its approval for this study.

Cell culture

Human colon cancer cell lines, Caco2/bbe, HT-29, SKCO-1, SW480 and SW620, were purchased from the ATCC and grown in high-glucose Dulbecco's Modified Eagle's Medium (Caco2/bbe, HT-29, SKCO1) or Roswell Park Memorial Institute 1640 (SW480 and SW620) supplemented with 10% (vol/vol) fetal bovine serum, 2 mM of L-glutamine, 50 U/ml of penicillin, 50 μg/ml of streptomycin and 10 μg/ml of transferrin (all purchased from Invitrogen/GIBCO, Grand Island, NY, USA) in a humidified atmosphere of 5% CO_2. The cells were plated on 6- or 12-well plates at a density of 10^5 cells/cm^2.

Protein extraction

The total proteins were extracted from samples using a Mammalian Cell Extraction Kit (BioVision, Mountain View, CA, USA). The cells were lysed for immunoprecipitation using Buffer A (10 mM of Tris-Cl, pH 7.9, 60 mM of KCl, 1 mM of EDTA and 1 mM of dithiothreitol) containing 0.1% Nonidet P-40, 1 mM of phenylmethylsulfonyl fluoride and a complete protease inhibitor (Roche Molecular Biochemicals, Indianapolis, IN, USA). To obtain proteins from the cytosolic organelles, the cells were lysed in gradient buffer (0.25 M sucrose, 20 mM of HEPES (pH 7.0), 0.02% sodium azide and a complete protease inhibitor) and then homogenized using a needle. The cell suspensions were centrifuged for 5 min at 1200 r.p.m., and the supernatants were harvested as cytosolic organelle samples. The cells were lysed using cytosol lysis buffer (10 mM of HEPES-KOH (pH 7.8), 10 mM of KCl, 0.1 mM of EDTA, RNase inhibitor (Applied Biosystems, Foster City, CA, USA, 40 units/ml) and complete protease cocktail) and nucleus lysis buffer (50 mM HEPES-KOH (pH 7.8), 420 mM of KCl, 0.1 mM of EDTA, 5 mM of $MgCl_2$, 20% Glycerol, RNase inhibitor (40 units/ml) and complete protease cocktail) in order to separately extract the proteins from the cytosol and nucleus. The cells were washed with PBS and lysed in cytosol lysis buffer before being subjected to five minutes of incubation, followed by five minutes of centrifugation at 1200 r.p.m., and the supernatants were harvested. The pellets were then resuspended in cytosol lysis buffer and centrifuged again. Finally, the pellets were gently resuspended in nuclear lysis buffer and used as the nucleoplasmic fraction.

Inhibitors

MG132 (ENZO Life Science Inc., Farmingdale, NY, USA) or 3-Methiladenine (R&D systems, Minneapolis, MN, USA) was used to inhibit the proteasomal or autophagosomal degradation of proteins, respectively.

Plasmids, RNAs and transfections

cDNA was obtained using reverse transcription (RT)-PCR of SW620 cells with a high-capacity cDNA reverse transcription kit (Applied Biosystems). hnRNP A1 DNA was amplified using PCR with a primer set in which the 5′ end of the upstream region contained the *Nhe*I restriction site, and the downstream region contained the *Bam HI* restriction site (sense, 5′-agtcagctagccttcaccctgccgtcatg-3′, anti-sense, 5′-agtcaggatcccctgctaag ctttgtttcc-3′). The *Nhe*I/*Bam HI* digested PCR product was cloned into the multicloning site of the pIRES puro2 vector (CLONTECH Laboratories, Inc., Mountain View, CA, USA). RNAs were synthesized by Hokkaido System Science Co., Ltd. The nucleotide sequences of the miR-18a duplex were: sense, 5′-uaaggugcaucuagugcagaua-3′ and antisense, 5′-acugcccuaagug-cuccuucu-3′. A negative control with a scrambled miRNA sequence was prepared by annealing two synthetic RNAs: sense, 5′-uacguacuaucgcgcg-gau-3′ and antisense, 5′-auccgcgcgauaguacgua-3′. siRNAs for hnRNP A1 and BAG3 and siRNAs for ATG7 and SQSTM1/p62 were purchased from Santa Cruz Biotechnology (Santa Cruz, CA, USA) and Cell Signaling Technology, Inc. (Danvers, MA, USA) respectively. The cells were seeded 24 h prior to transfection, and transfection was performed using the HVJ Envelope VECTOR KIT (Ishihara Sangyo, Osaka, Japan).

Lentiviruses and infections

The lentivirus containing the whole sequence of the target microRNA (control and miR-18a) was purchased from Applied Biological Materials,

Inc. (Richmond, BC, Canada) Cells were grown in culture media containing polybrane (Santa Cruz Biotechnology) with the lentivirus vector and were selected in media containing 5 μg/ml puromycin. Cells with the lentivirus vector containing the whole sequence of the target microRNA were used for the xenograft model.

Immunoprecipitation

Each lysate sample was immunoprecipitated using IgG, hnRNP A1 or FITC antibodies (1 μg each), then 30 μl of protein G Sepharose 4 Fast Flow (GE Healthcare, Buckinghamshire, UK) was added. The mixtures were incubated overnight at 4°C, washed three times with PBS and boiled in Laemmli buffer to extract the proteins.

Western blot analyses

Equal amounts of protein were resolved using SDS–PAGE (12.5%), blotted onto a nitrocellulose membrane and then blocked in PBS with 0.05% (vol/vol) Tween 20 (T-PBS) containing 1% (wt/vol) bovine serum albumin. The blot was incubated overnight at 4°C with primary antibodies. The monoclonal antibodies against hnRNP A1 (Novus Biologicals, Littleton, CO, USA), RUNX 1 (Novus Biologicals), FITC (Novus Biologicals), ATG7 (Cell Signaling Technology), cyclin D1 (Santa Cruz Biotechnology), cyclin D2 (Abcam, Tokyo, Japan), NEDD9 (Abcam), estrogen receptor α (Abcam) and CD166 (Abcam), and the polyclonal antibodies against SQSTM1/p62 (Novus Biologicals), IGF1 (Abcam), BAG3 (Abnova), LC-3 (Medical & Biological Laboratories co., Ltd, Nagoya, Japan) and PTP4A3 (Abcam) were used as primary antibodies. The blots were then washed in T-PBS, incubated with a HRP-conjugated secondary antibody (R&D Systems), washed in T-PBS and then developed using either the Super-Signal West Pico or the femto enhanced chemiluminescence system (Thermo science, Waltham, MA, USA). The average protein expression was normalized to the actin expression (BD transduction laboratories, Lexington, KY, USA).

Real-time PCR

Total RNA was extracted using an RNeasy mini kit (Qiagen, Tokyo, Japan) according to the manufacturer's instructions. The mRNAs were reverse transcribed using a high-capacity cDNA reverse transcription kit (Applied Biosystems). The gene expression was measured using specific primers (hnRNP A1: sense, 5′-tcgtcagcttgctccttttctg-3′, anti-sense, 5′-atgacggcag ggtgaagaga-3′, taqman probe, 5′-ccgccgaagaagcatcgttaaagt-3′; CTGF: sense, 5′-tgtgtgacgagcccaagga-3′, anti-sense, 5′-tctgggccaaacgtgtcttc-3′, taqman probe, 5′-tggttgggcctgccctcgc-3′) in triplicate. The average mRNA expression was normalized to the 18S rRNA expression (Applied Biosystems).

Binding assay

The cells were lysed using lysis buffer A (10 mM of Tris-Cl, pH 7.9, 60 mM of KCl, 1 mM of EDTA and 1 mM of dithiothreitol) containing 0.1% Nonidet P-40, 1 mM of phenylmethylsulfonyl fluoride and complete protease inhibitors. The lysates were clarified by centrifugation for 10 min at 12 000 r.p.m., and an RNase inhibitor (40 units/ml) was added. The cell lysates were immunoprecipitated using IgG or hnRNP A1 antibodies (1 μg each) and 30 μl of protein G Sepharose 4 Fast Flow. RNA was extracted from the beads using phenol-chloroform extraction and was reverse-transcribed using a taqman microRNA reverse transcription kit (Applied Biosystems). The resulting cDNA was measured using real-time PCR for hsa-miR-18a (Applied Biosystems).

Immunocytochemistry

The cells were plated on chamber slides, which were fixed in 4% paraformaldehyde, washed extensively with PBS, permeabilized with 0.1% Triton X-100 and blocked in 3% BSA in PBS. The slides were then sequentially incubated with primary antibodies, washed with PBS and incubated with Alexa 488 and/or 594-conjugated secondary antibodies (Invitrogen-Molecular Probes, Carlsbad, CA, USA). The nuclei were counterstained with DAPI (Lonza, Tokyo, Japan). The cells were mounted with an anti-fade mounting medium, and the immunofluorescence was visualized using a fluorescence microscope (KEYENCE corporation, Osaka, Japan).

Telomere length assay

The cells were washed with PBS and incubated with lysis buffer (25 mM of Tris-HCl (pH 8.0), 50 mM of EDTA (pH 8.0) 1% SDS) 400 μl/sample, 10 mg/ml of protein kinase K 10 μl/sample) at 55°C overnight. DNA was extracted using phenol-chloroform extraction and was dissolved in distilled water. The telomere length was detected using a TeloTTAGGG telomere length assay (Roche Applied Science, Penzberg, Germany) according to the manufacturer's instructions.

MTT assay

The cells were seeded on 96-well microplates at 1.0×10^4 per well 24 h prior to transfection. The cell growth was assessed using an MTT cell proliferation kit according to the manufacturer's instructions (Roche Applied Science). The optical density was measured at a 590 nm test wavelength and a 620 nm reference wavelength.

Radioactive materials

The [^{3}H]-glycine and [^{14}C]-glycine were purchased from PerkinElmer, Japan.

Isotope studies

Each group of cells in the single isotope study was treated with [^{3}H]-glycine for 24 h. Next, the complex of expression vectors of hnRNP A1 and double-stranded miR-18a enclosed using the HVJ Envelope VECTOR KIT was added to the cells. In the other set of experiments, each group of mice in the double isotope study received vectors encoding hnRNP A1 and double-stranded miR-18a and were injected with 100 μCi of [^{3}H]-glycine 3 h later. Each group was given a booster injection of an expression vector for hnRNP A1 again after an additional 72 h. Thereafter, the mice were injected with 12.5 μCi of [14C]-glycine 3 h later, and then killed 3 h after that. Protein samples were collected from the intestines using lysis buffer A and were analyzed by immunoprecipitation with hnRNP A1 antibodies. The radioactivity was measured in a Beckman scintillation spectrometer.

Xenografts

The protocols for the animal experiments were approved by the Asahikawa Medical University Institutional Animal Care and Use Committee. SW620 cells (1×10^6 cells) were injected into male BALB/c nude mice. Double-stranded miR-18a or control RNA was transfected daily starting one week after the injection of SW620 cells for tumor treatment.

CONFLICT OF INTEREST

The authors declare no conflicts of interest.

REFERENCES

1 Capon DJ, Seeburg PH, McGrath JP, Hayflick JS, Edman U, Levinson AD *et al.* Activation of Ki-ras2 gene in human colon and lung carcinomas by two different point mutations. *Nature* 1983; **304**: 507–513.
2 Forrester K, Almoguera C, Han K, Grizzle WE, Perucho M. Detection of high incidence of K-ras oncogenes during human colon tumorigenesis. *Nature* 1987; **327**: 298–303.
3 Guan RJ, Fu Y, Holt PR, Pardee AB. Association of K-ras mutations with p16 methylation in human colon cancer. *Gastroenterology* 1999; **116**: 1063–1071.
4 Nigro JM, Baker SJ, Preisinger AC, Jessup JM, Hostetter R, Cleary K *et al.* Mutations in the p53 gene occur in diverse human tumour types. *Nature* 1989; **342**: 705–708.
5 Powell SM, Zilz N, Beazer-Barclay Y, Bryan TM, Hamilton SR, Thibodeau SN *et al.* APC mutations occur early during colorectal tumorigenesis. *Nature* 1992; **359**: 235–237.
6 Taft RJ, Pang KC, Mercer TR, Dinger M, Mattick JS. Non-coding RNAs: regulators of disease. *J Pathol* 2010; **220**: 126–139.
7 Mattick JS, Gagen MJ. The evolution of controlled multitasked gene networks: the role of introns and other noncoding RNAs in the development of complex organisms. *Mol Biol Evol* 2001; **18**: 1611–1630.
8 Bartel DP. MicroRNAs: genomics, biogenesis, mechanism, and function. *Cell* 2004; **116**: 281–297.
9 Winter J, Jung S, Keller S, Gregory RI, Diederichs S. Many roads to maturity: microRNA biogenesis pathways and their regulation. *Nat Cell Biol* 2009; **11**: 228–234.
10 Eulalio A, Huntzinger E, Izaurralde E. Getting to the root of miRNA-mediated gene silencing. *Cell* 2008; **132**: 9–14.

11 Filipowicz W, Bhattacharyya SN, Sonenberg N. Mechanisms of post-transcriptional regulation by microRNAs: are the answers in sight? *Nat Rev Genet* 2008; **9**: 102–114.
12 Lee RC, Feinbaum RL, Ambros V. The C. elegans heterochronic gene lin-4 encodes small RNAs with antisense complementarity to lin-14. *Cell* 1993; **75**: 843–854.
13 Wienholds E, Kloosterman WP, Miska E, Alvarez-Saavedra E, Berezikov E, de Bruijn E *et al.* MicroRNA expression in zebrafish embryonic development. *Science* 2005; **309**: 310–311.
14 Wightman B, Ha I, Ruvkun G. Posttranscriptional regulation of the heterochronic gene lin-14 by lin-4 mediates temporal pattern formation in C. elegans. *Cell* 1993; **75**: 855–862.
15 Calin GA, Dumitru CD, Shimizu M, Bichi R, Zupo S, Noch E *et al.* Frequent deletions and down-regulation of micro- RNA genes miR15 and miR16 at 13q14 in chronic lymphocytic leukemia. *Proc Natl Acad Sci USA* 2002; **99**: 15524–15529.
16 He L, Thomson JM, Hemann MT, Hernando-Monge E, Mu D, Goodson S *et al.* A microRNA polycistron as a potential human oncogene. *Nature* 2005; **435**: 828–833.
17 Johnson SM, Grosshans H, Shingara J, Byrom M, Jarvis R, Cheng A *et al.* RAS is regulated by the let-7 microRNA family. *Cell* 2005; **120**: 635–647.
18 Ventura A, Young AG, Winslow MM, Lintault L, Meissner A, Erkeland SJ *et al.* Targeted deletion reveals essential and overlapping functions of the miR-17 through 92 family of miRNA clusters. *Cell* 2008; **132**: 875–886.
19 Sampson VB, Rong NH, Han J, Yang Q, Aris V, Soteropoulos P *et al.* MicroRNA let-7a down-regulates MYC and reverts MYC-induced growth in Burkitt lymphoma cells. *Cancer Res* 2007; **67**: 9762–9770.
20 Liu WH, Yeh SH, Lu CC, Yu SL, Chen HY, Lin CY *et al.* MicroRNA-18a prevents estrogen receptor-alpha expression, promoting proliferation of hepatocellular carcinoma cells. *Gastroenterology* 2009; **136**: 683–693.
21 Zhao Y, Deng C, Wang J, Xiao J, Gatalica Z, Recker RR *et al.* Let-7 family miRNAs regulate estrogen receptor alpha signaling in estrogen receptor positive breast cancer. *Breast Cancer Res Treat* 2011; **127**: 69–80.
22 Tao J, Wu D, Li P, Xu B, Lu Q, Zhang W. microRNA-18a, a member of the oncogenic miR-17-92 cluster, targets Dicer and suppresses cell proliferation in bladder cancer T24 cells. *Mol Med Rep* 2012; **5**: 167–172.
23 Motoyama K, Inoue H, Takatsuno Y, Tanaka F, Mimori K, Uetake H *et al.* Over- and under-expressed microRNAs in human colorectal cancer. *Int J Oncol* 2009; **34**: 1069–1075.
24 Eiring AM, Harb JG, Neviani P, Garton C, Oaks JJ, Spizzo R *et al.* miR-328 functions as an RNA decoy to modulate hnRNP E2 regulation of mRNA translation in leukemic blasts. *Cell* 2010; **140**: 652–665.
25 Guil S, Caceres JF. The multifunctional RNA-binding protein hnRNP A1 is required for processing of miR-18a. *Nat Struct Mol Biol* 2007; **14**: 591–596.
26 Michlewski G, Guil S, Semple CA, Caceres JF. Posttranscriptional regulation of miRNAs harboring conserved terminal loops. *Molecular cell* 2008; **32**: 383–393.
27 Ushigome M, Ubagai T, Fukuda H, Tsuchiya N, Sugimura T, Takatsuka J *et al.* Up-regulation of hnRNP A1 gene in sporadic human colorectal cancers. *Int J Oncol* 2005; **26**: 635–640.
28 Thiele BJ, Doller A, Kahne T, Pregla R, Hetzer R, Regitz-Zagrosek V. RNA-binding proteins heterogeneous nuclear ribonucleoprotein A1, E1, and K are involved in post-transcriptional control of collagen I and III synthesis. *Circ Res* 2004; **95**: 1058–1066.
29 Jo OD, Martin J, Bernath A, Masri J, Lichtenstein A, Gera J. Heterogeneous nuclear ribonucleoprotein A1 regulates cyclin D1 and c-myc internal ribosome entry site function through Akt signaling. *J Biol Chem* 2008; **283**: 23274–23287.
30 Kirkin V, McEwan DG, Novak I, Dikic I. A role for ubiquitin in selective autophagy. *Molecular cell* 2009; **34**: 259–269.
31 Kettern N, Rogon C, Limmer A, Schild H, Hohfeld J. The Hsc/Hsp70 co-chaperone network controls antigen aggregation and presentation during maturation of professional antigen presenting cells. *PLoS One* 2011; **6**: e16398.
32 Yamakuchi M, Lotterman CD, Bao C, Hruban RH, Karim B, Mendell JT *et al.* P53-induced microRNA-107 inhibits HIF-1 and tumor angiogenesis. *Proc Natl Acad Sci USA* 2010; **107**: 6334–6339.
33 Tsuchiya N, Izumiya M, Ogata-Kawata H, Okamoto K, Fujiwara Y, Nakai M *et al.* Tumor suppressor miR-22 determines p53-dependent cellular fate through post-transcriptional regulation of p21. *Cancer Res* 2011; **71**: 4628–4639.
34 Zhang Y, Wang Z, Chen M, Peng L, Wang X, Ma Q *et al.* MicroRNA-143 targets MACC1 to inhibit cell invasion and migration in colorectal cancer. *Mol Cancer* 2012; **11**: 23.
35 Wu J, Wu G, Lv L, Ren YF, Zhang XJ, Xue YF *et al.* MicroRNA-34a inhibits migration and invasion of colon cancer cells via targeting to Fra-1. *Carcinogenesis* 2012; **33**: 519–528.
36 Yu Y, Kanwar SS, Patel BB, Oh PS, Nautiyal J, Sarkar FH *et al.* MicroRNA-21 induces stemness by downregulating transforming growth factor beta receptor 2 (TGFbetaR2) in colon cancer cells. *Carcinogenesis* 2012; **33**: 68–76.
37 Hope NR, Murray GI. The expression profile of RNA-binding proteins in primary and metastatic colorectal cancer: relationship of heterogeneous nuclear ribonucleoproteins with prognosis. *Hum Pathol* 2011; **42**: 393–402.
38 Qased AB, Yi H, Liang N, Ma S, Qiao S, Liu X. MicroRNA-18a upregulates autophagy and ataxia telangiectasia mutated gene expression in HCT116 colon cancer cells. *Mol Med Report* 2013; **7**(2): 559–564.

Supplementary Information accompanies this paper on the Oncogene website (http://www.nature.com/onc)

Hepatology Research

Hepatology Research 2014; 44: 920–934 doi: 10.1111/hepr.12199

Original Article

Augmented hepatic Toll-like receptors by fatty acids trigger the pro-inflammatory state of non-alcoholic fatty liver disease in mice

Koji Sawada,[1] Takaaki Ohtake,[1] Takumu Hasebe,[1] Masami Abe,[1] Hiroki Tanaka,[2] Katsuya Ikuta,[1] Yasuaki Suzuki,[4] Mikihiro Fujiya,[1] Chitomi Hasebe[3] and Yutaka Kohgo[1]

[1]*Department of Medicine, Division of Gastroenterology and Hematology/Oncology,* [2]*Department of Gastrointestinal Immunology and Regenerative Medicine, Asahikawa Medical University,* [3]*Department of Gastroentelorogy, Asahikawa Red Cross Hospital, Asahikawa, and* [4]*Department of Gastroenterology, Nayoro City General Hospital, Nayoro, Japan*

Aim: There is considerable evidence that intestinal microbiota are involved in the development of metabolic syndromes and, consequently, with the development of non-alcoholic fatty liver disease (NAFLD). Toll-like receptors (TLRs) are essential for the recognition of microbiota. However, the induction mechanism of TLR signals through the gut-liver axis for triggering the development of non-alcoholic steatohepatitis (NASH) or NAFLD remains unclear. In this study, we investigated the role of palmitic acid (PA) in triggering the development of a pro-inflammatory state of NAFLD.

Methods: Non-alcoholic fatty liver disease was induced in mice fed a high fat diet (HFD). The mice were killed and the expression of TLRs, tumor necrosis factor (TNF), interleukin (IL)-1β, and phospho-interleukin-1 receptor-associated kinase 1 in the liver and small intestine were assessed. In addition, primary hepatocytes and Kupffer cells were treated with PA, and the direct effects of PA on TLRs induction by these cells were evaluated.

Results: The expression of inflammatory cytokines such as TNF, IL-1β, and TLR-2, -4, -5, and -9 was increased in the liver, but decreased in the small intestine of HFD-fed mice *in vivo*. In addition, the expression of TLRs in primary hepatocytes and Kupffer cells was increased by treatment with PA.

Conclusion: In the development of the pro-inflammatory state of NAFLD, PA triggers the expression of TLRs, which contribute to the induction of inflammatory cytokines through TLR signals by intestinal microbiota.

Key words: fatty acids, gut-liver axis, non-alcoholic fatty liver disease, pro-inflammatory state, Toll-like receptor

INTRODUCTION

NON-ALCOHOLIC FATTY LIVER disease (NAFLD) is a form of steatosis with or without inflammation of the liver, and it is not related to excessive alcohol intake. NAFLD includes both simple steatosis and non-alcoholic steatohepatitis (NASH), the latter developing further into cirrhosis and hepatocellular carcinoma.[1] NAFLD is one of the most common liver diseases worldwide and is considered to be related to obesity, insulin resistance, and metabolic syndrome.[2]

A two-hit theory has been proposed to explain the pathogenesis of NASH.[3] First, simple steatosis is induced by obesity and insulin resistance. Second, NASH develops by several hits, including adipocytokines, iron, and bacterial endotoxins/lipopolysaccharide (LPS) derived from gram-negative bacteria.[4–6]

Toll-like receptors (TLRs) recognize pathogen- and endogenous damage-associated molecular patterns and activate nuclear factor-κB (NF-κB), which induces pro-inflammatory cytokines/chemokines and type 1 interferon through phosphorylation of interleukin-1 receptor-associated kinase 1 (IRAK1) and IRAK4.[7] Therefore, TLRs may play important roles in the activation of innate immunity. Among TLRs, TLR2, TLR4, TLR5, and

Correspondence: Dr Takaaki Ohtake, Department of Medicine, Division of Gastroenterology and Hematology/Oncology, Asahikawa Medical University, 2-1 Midorigaoka Higashi, Asahikawa 078-8510, Japan. Email: totake@asahikawa-med.ac.jp
Received 30 January 2013; revision 18 June 2013; accepted 1 July 2013.

TLR9 were identified as bacterial recognition receptors capable of recognizing lipopeptide, LPS, flagellin, and CpG-DNA, respectively.[8] Recently it was reported that TLR signal pathways, the ligands of which are bacterial components, play an important role in the pathogenesis of alcoholic liver disease and NASH.[9] In particular, the association between TLR4 signal pathways and the development of NASH was investigated.[6,10,11] More recently, Miura *et al.* reported decreased levels of steatohepatitis and liver fibrosis in TLR9 knockout mice compared with those in wild-type mice in a choline-deficient amino acid-defined (CDAA) diet-induced NASH model.[12] In contrast, in TLR2-deficient mice fed a methionine- and choline-deficient (MCD) diet, an increased level of liver injury was noted, suggesting a potential protective role of TLR2 in fatty liver.[6]

An increasing proportion of the general population suffers from obesity, which is an emerging global problem along with its related disorders such as metabolic syndrome. Much recent evidence shows that microbiota are associated with these conditions.[13–19] In the intestine, TLRs are typically expressed in the epithelial cells and are involved in the production of immunoglobulin A (IgA), maintenance of tight junctions, proliferation of epithelial cells, and expression of antimicrobial peptides.[20] TLR5, which specifically recognizes flagellin, is involved in promoting the pathophysiology of inflammatory bowel disease.[21] While the above reports suggest that intestinal TLRs play an important role in innate immunity of the gut, the association between their role in the small intestine and that in the development of NASH remains unclear.

The present study was based on hypernutrition and obesity and evaluated the significance of TLRs and their signaling in the liver and small intestine using a high-fat diet (HFD)-induced NAFLD mouse model. In addition, a gut-sterilized mouse model treated with antibiotics was used to confirm whether there is an association between intestinal microbiota and TLR expression.

METHODS

Animal studies

IN THE HFD group, 8-week-old male C57BL/6J mice (Charles River Japan, Tokyo, Japan) were fed a HFD containing 60% triglycerides with oleic acid (OA), palmitic acid (PA), and stearic acid (Table 1) (F2HFD2; Oriental Yeast Company, Tokyo, Japan). Control mice were fed a diet containing 5% triglycerides (MF; Oriental Yeast Company). All mice were maintained under controlled conditions (22°C; humidity, 50–60%, 12-h light/dark cycle) with food and water *ad libitum*. Mice from both groups were killed at 4, 8, and 16 weeks for blood and tissue collection. These animals were fasted for 10-h before blood and tissue collection. After each mouse was anesthetized with diethyl ether and weighed, blood was collected by a cardiac puncture and subsequently assayed for biochemical parameters. The liver and small intestine were dissected, weighed, and frozen in liquid nitrogen. These samples were used later for histological and polymerase chain reaction (PCR) analysis. All experiments were performed in accordance with the rules and guidelines of the Animal Experiment Committee of Asahikawa Medical University.

Table 1 Composition of fatty acids in control diet and high fat diet

	Control diet (%)	High fat diet (%)
Oleic acid	No detect	30
Palmitic acid	No detect	25
Stearic acid	0.22	16
Palmitoleic acid	0.05	2.0
Myristic acid	0.03	1.5

Isolation and primary culture of hepatocytes and Kupffer cells

Mouse hepatocytes and Kupffer cells were isolated using a modified collagenase perfusion method.[22] Briefly, the liver was perfused via the portal vein with Ca^{2+} and Mg^{2+} free Hank's balanced salt solution (HBSS(−)) at 39°C for 5 min at 10 mL/min, followed by HBSS(+) for 5 min at 10 mL/min supplemented with 0.05% collagenase (Wako, Tokyo, Japan). The liver was then removed, fragmented and vortexed for a few seconds. After filtration with mesh, the cell suspension was centrifuged at 500 rpm for 1 min. The cells in the pellet were minced twice and used as primary hepatocytes for culture in William's E medium with epidermal growth factor (5 μg), insulin (5 mg), L-glutamine, penicillin, streptomycin, and 10% fetal bovine serum (FBS). The supernatant was centrifuged at 500 rpm for 1 min at three to four times to remove any remaining hepatocytes. The supernatant was then minced twice and cultured in Dulbecco's modified Eagle's medium with penicillin, streptomycin, and 10% FBS. After 60 min, adhesion cells were used as Kupffer cells.

PA treatment

Isolated hepatocytes and Kupffer cells were treated with PA. PA complexed with 1% bovine serum albumin

(BSA) was added to the medium to attain final concentrations of 10 μM and 100 μM over 24 h.

Fat droplet evaluation

4,4-difluoro-1,3,5,7,8-pentamethyl-4-bora-3a,4a-diazas-indacene (BODIPY 493/503, Invitrogen, Carlsbad, CA, USA) was added as a lipid probe overnight to the culture medium and fluorescent images were observed.

Biochemical analyses

Serum alanine aminotransferase (ALT) and free fatty acids were measured using the Automatic Analyzer 7180 (Hitachi High-Technologies Corporation, Tokyo, Japan).

Histopathological evaluation

Samples of remaining liver tissue were fixed in 10% formalin buffer, embedded in paraffin, sectioned, and stained with hematoxylin and eosin (H&E).

RNA isolation and first strand complementary DNA synthesis

Total RNA was isolated from the liver, small intestine, primary hepatocytes, and Kupffer cells using QIAGEN RNeasy Mini Kit (QIAGEN, Hilden, Germany). RNA was reverse-transcribed by RETROscript using Random decamers (Ambion, Austin, TX, USA). Detailed methods were performed according to the manufacturers' instructions.

Primer pairs of TLR-related molecules

Mouse 18srRNA was used as an endogenous amplification control. The use of this universally expressed housekeeping gene allows for correction of variations in the efficiency of RNA extraction and reverse transcription. TaqMan assays were used for specific primer and probe sets on TLR2, TLR4, TLR5, TLR9, tumor necrosis factor (TNF), interleukin (IL)-1β, and 18srRNA (Applied Biosystems, Foster City, CA, USA).

Quantitative real-time PCR

The expression of TLR2, TLR4, TLR5, TLR9, IL-1β, and TNF in mouse liver, small intestine, primary hepatocytes, and Kupffer cells was evaluated by quantitative real-time PCR (qPCR) (7300 Real-time PCR system; Applied Biosystems). In this method, all reactions were run in 96-well plates with a total volume of 20 μL. The reaction mixture consisted of 10 μL TaqMan Universal PCR Master mix, 1 μL 18srRNA, 1 μL primer, 5 μL RNAase free water, and 3 μL complementary DNA. The PCR reaction involved the following steps: (i) 50°C for 2 min to prevent carryover of DNA, (ii) 95°C for 10 min to activate polymerase, and (iii) 40 cycles each of 95°C for 15 s, 60°C for 15 s, and 72°C for 45 s. qPCR data were analyzed by the comparative CT method.

Immunohistochemistry/ immunocytochemistry

Immunohistochemistry using F4/80 as a macrophage marker was performed on cryostatically sectioned liver and staining was performed by immunofluorescence. The sections were fixed in 2% paraformaldehyde for 10 min and washed three times with PBS for 5 min. Furthermore, sections for F4/80 were blocked with 3% BSA/PBS for 1 h at room temperature, followed by incubation with monoclonal antibody against F4/80 (Abcam, Cambridge, MA, USA) 1:100 diluted in 3% BSA/PBS for 1 h at room temperature. After washing, F4/80 slides were incubated with 1:200 diluted Alexa Fluor 488 goat anti-rat IgG (Invitrogen) for 1 h at room temperature and washed.

Immunocytochemical staining was also performed using the immunofluorescence method. After the chamber slides in which primary Kupffer cells had been cultured were washed twice with PBS for 5 min, primary Kupffer cells were fixed in 2% paraformaldehyde for 20 min and washed twice with PBS for 5 min. Primary Kupffer cells were then incubated with 0.1% Triton X-100 in PBS for 2 min to permeabilize the membranes and washed twice with PBS. The slides for phospho-interleukin-1 receptor-associated kinase1 (pIRAK1; Abcam) were blocked with 3% BSA/PBS for 1 h at room temperature, followed by incubation with monoclonal antibody against pIRAK1 diluted 1:500 in 3% BSA/PBS for 1 h at room temperature. After washing, the slides were incubated with 1:500 diluted Alexa Fluor 594 goat anti-rat IgG (Invitrogen) for 1 h at room temperature and washed.

Western blotting analysis

Protein expression of pIRAK1, the key mediator in the TLR signaling pathway,[23] in the liver (30 μg), small intestine (30 μg) was studied by Western blot analysis. Protein concentrations were measured by the Bradford method using the Pierce BCA Protein Assay kit (Thermo Scientific, Rockford, IL, USA) according to the manufacturer's instructions. Separation of 30 μg of protein was then performed by 12% Mini PROTEAN TGX Precast Gels (Bio-Rad, Hercules, CA, USA). After electrophoresis, proteins were transferred to nitrocellulose membranes (Amersham Life Science Piscataway, NJ, USA),

blocked in 5% skim milk, and 0.2% Tween20 in PBS (PBS-T) for 1 h at room temperature, reacted overnight at 4°C with either rabbit polyclonal anti-pIRAK1 (Abcam) or β-actin (BD Biosciences) as a control, washed with 0.2% PBS-T, reacted with secondary antibody horseradish peroxidase-conjugated anti-rabbit IgG and anti-mouse IgG (RD, Minneapolis, MN, USA) for 1 h, and washed with PBS-T. After reaction with horseradish peroxidase-conjugated anti-rabbit and anti-mouse IgG, immune complexes were visualized by Super Signal West Pico Chemoluminescent Substrate (Thermo Scientific) according to the manufacturer's suggested procedure. pIRAK1 was analyzed by Image J software under the area, which compensated for β-actin.

Statistical analysis

The results are expressed as mean ± standard error, with the two groups being analyzed by Student's *t*-test and datasets involving more than two groups being analyzed by analysis of variance (ANOVA). *P*-values of <0.05 were considered statistically significant.

Gut sterilization

Mice were treated with ampicillin (1 g/L; Sigma-Aldrich, St. Louis, MO, USA), neomycin (1 g/L; Sigma), metronidazole (1 g/L; Sigma), and vancomycin (500 mg/L; Sigma) in drinking water for 8 weeks.[24] This treatment was followed by feeding with HFD for further 8 weeks.

RESULTS

Fatty liver in HFD-fed mice

AT 16 WEEKS, body weight and serum ALT levels were significantly higher in the HFD-fed mice (group F) than in those fed the control diet (group C) (body weight: C, 41.6 g; F, 51.0 g; serum ALT: C, 34 IU/L; F, 180 IU/L; Fig. 1a,b). Histopathological liver findings from group F demonstrated the absence of fat droplets at 4 weeks (Fig. 1c). However, the deposition of micronodular fat droplets in the centrilobular zone (Fig. 1d) was observed at 8 weeks and macronodular fat droplets and ballooning degeneration (Fig. 1e) were observed at 16 weeks, without any obvious infiltration of inflammatory cells. F4/80 staining for macrophage markers did not demonstrate an increased number of Kupffer cells (Fig. 1f,g).

Upregulation of cytokines in the fatty liver of HFD-fed mice

Histopathological examination of livers from group F demonstrated no obvious infiltration of inflammatory cells, while mRNA levels of the inflammatory cytokines IL-1β and TNF were significantly higher at 16 weeks (Fig. 2a,b).

Upregulation of TLRs in the fatty liver of HFD-fed mice

To confirm whether TLRs expression contributes to the induction of the abovementioned cytokines, we analyzed the mRNA of TLR2, TLR4, TLR5, and TLR9 that recognize bacterial components in the liver. The expression of these TLRs in the liver was not different between the two groups at 4 and 8 weeks, but at 16 weeks, this was significantly higher in the F group than in the C group (Fig. 2c–f). Western blot analysis also demonstrated that the expression of pIRAK1 in the liver was significantly upregulated in the F group compared with that in the C group at 16 weeks (Fig. 2g). These findings suggest that TLR upregulation contributes to the induction of cytokines and that the TLR signal pathway is genetically enhanced in simple steatosis in the absence of inflammation.

Downregulation of TLRs and cytokines in the small intestine of HFD-fed mice

The expression of TLRs that recognize bacterial components was significantly upregulated in the NAFLD liver. Because liver injury has a connection with exposure to bacterial components of intestinal origin, we then examined the small intestine of the NAFLD model mice. The mRNA expression of small intestinal TLR2, TLR4, TLR5, and TLR9 was not significantly different between the two groups at 4 and 8 weeks. Histopathological examination of the small intestine revealed no difference between the groups at 16 weeks, but, mRNA expression of all four TLRs was significantly lower in the F group than in the C group at 16 weeks (Fig. 3a–d). Expression of IL-1β and TNF was also downregulated at 16 weeks (Fig. 3e,f). Moreover, pIRAK1 expression was also significantly decreased in the F group compared with that in the C group at 16 weeks (Fig. 3g). These findings indicate that the TLR signal pathway is genetically attenuated in the NAFLD small intestine.

Antibiotic treatment improved steatosis and TLRs expression in the liver of HFD-fed mice

Small intestinal bacterial overgrowth (SIBO) was reported to coexist with NASH,[14,25] and the following factors can predispose to SIBO: morbid obesity,[26] aging,[27] concurrent use of proton pump inhibitors,[28] and abnormal small intestinal motility.[29] Therefore, we hypothesized that attenuation of TLR signal

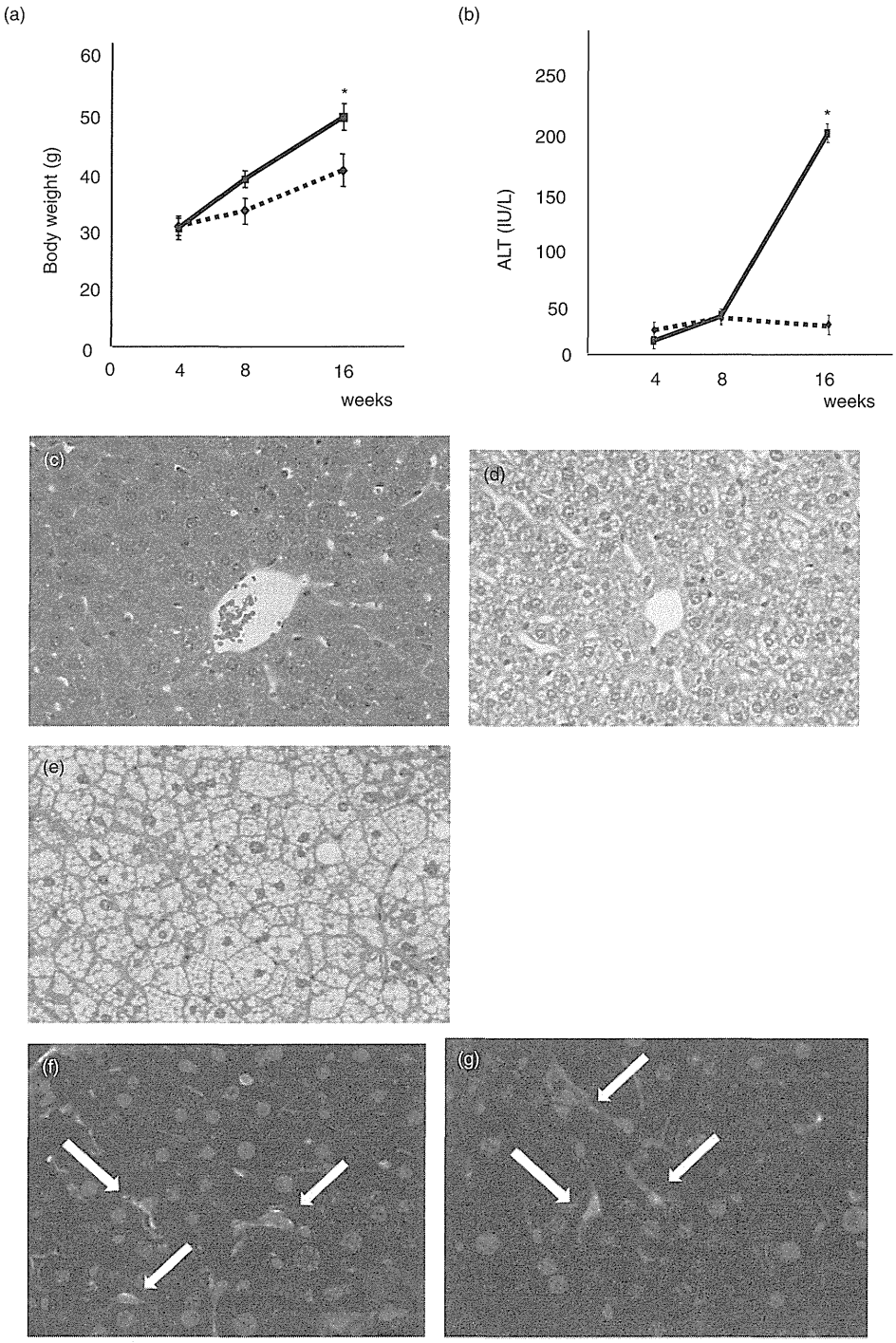

Figure 1 Body weight, serum alanine aminotransferase (ALT), and histopathological findings in high fat diet (HFD)-fed and control mice. Body weight (a) and serum ALT levels (b) were significantly higher in HFD-fed mice (F) than in controls at 16 weeks. Histopathological liver findings in F mice at 4, 8, and 16 weeks with H&E staining (×400, 4 weeks [c]; 8 weeks [d]; 16 weeks [e]). Micronodular fat droplets deposited in hepatocytes in the centrilobular zone at 8 weeks (d). Macronodular fat droplets and ballooning degeneration were marked at 16 weeks, but no obvious infiltration of inflammatory cells was observed (e). F4/80 staining for macrophage marker did not demonstrate any increase in Kupffer cells (control (f); 16 weeks (g); white arrows indicate Kupffer cells, × 400). (*$P < 0.05$).

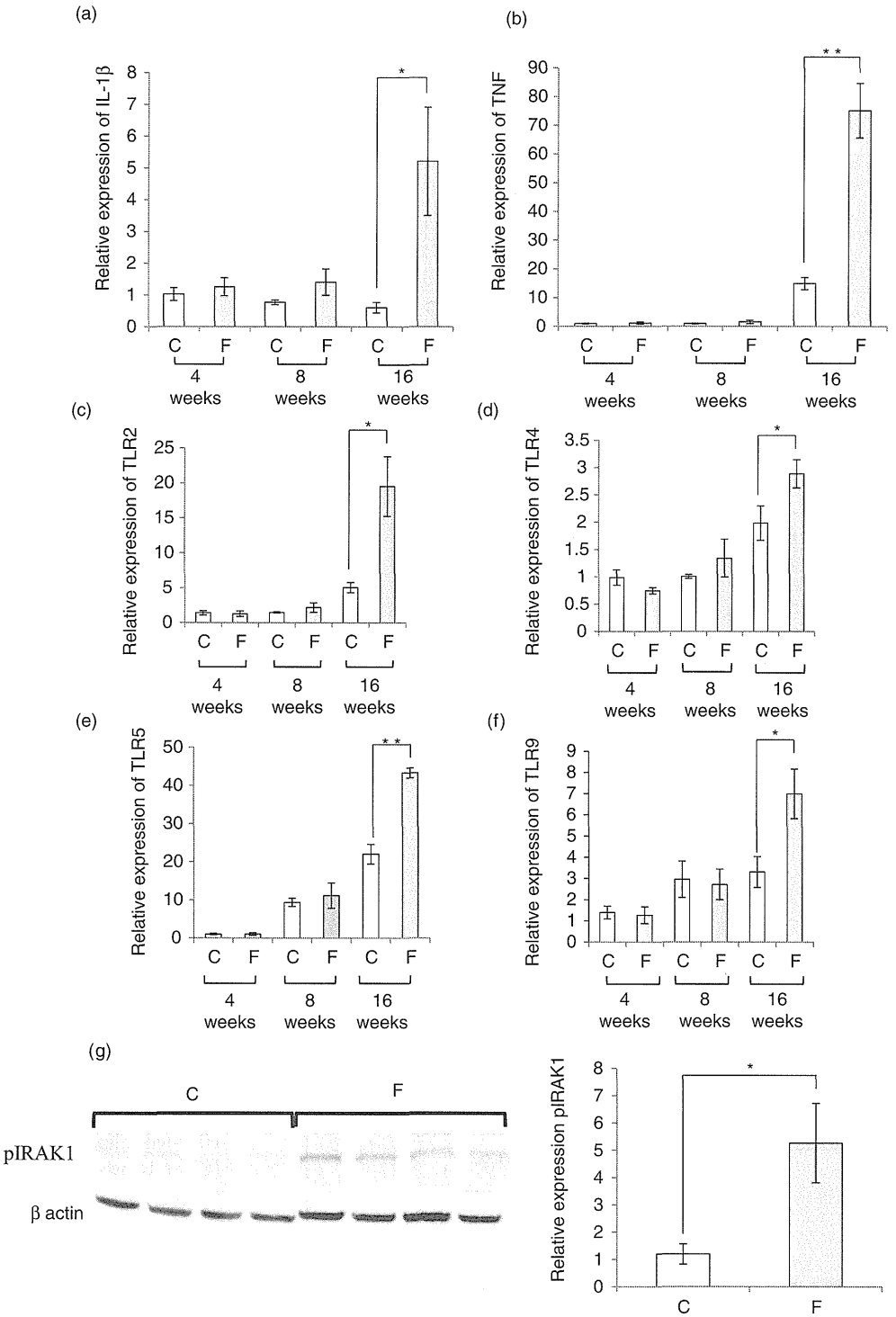

Figure 2 mRNA expression of inflammatory cytokines and Toll-like receptors in the liver of high fat diet (HFD)-fed and control mice. mRNA expression of interleukin (IL)-1β (a), and tumor necrosis factor (TNF) (b) was significantly higher in the liver of HFD-fed mice (F) than in that of controls (C) at 16 weeks. The expression of TLR2 (c), TLR4 (d), TLR5 (e), and TLR9 (f) mRNA was significantly higher in the liver in group F than in group C at 16 weeks. Western blot analysis demonstrated a higher expression of pIRAK1 in the liver in group F than in group C at 16 weeks (g). (*$P < 0.05$, **$P < 0.01$).

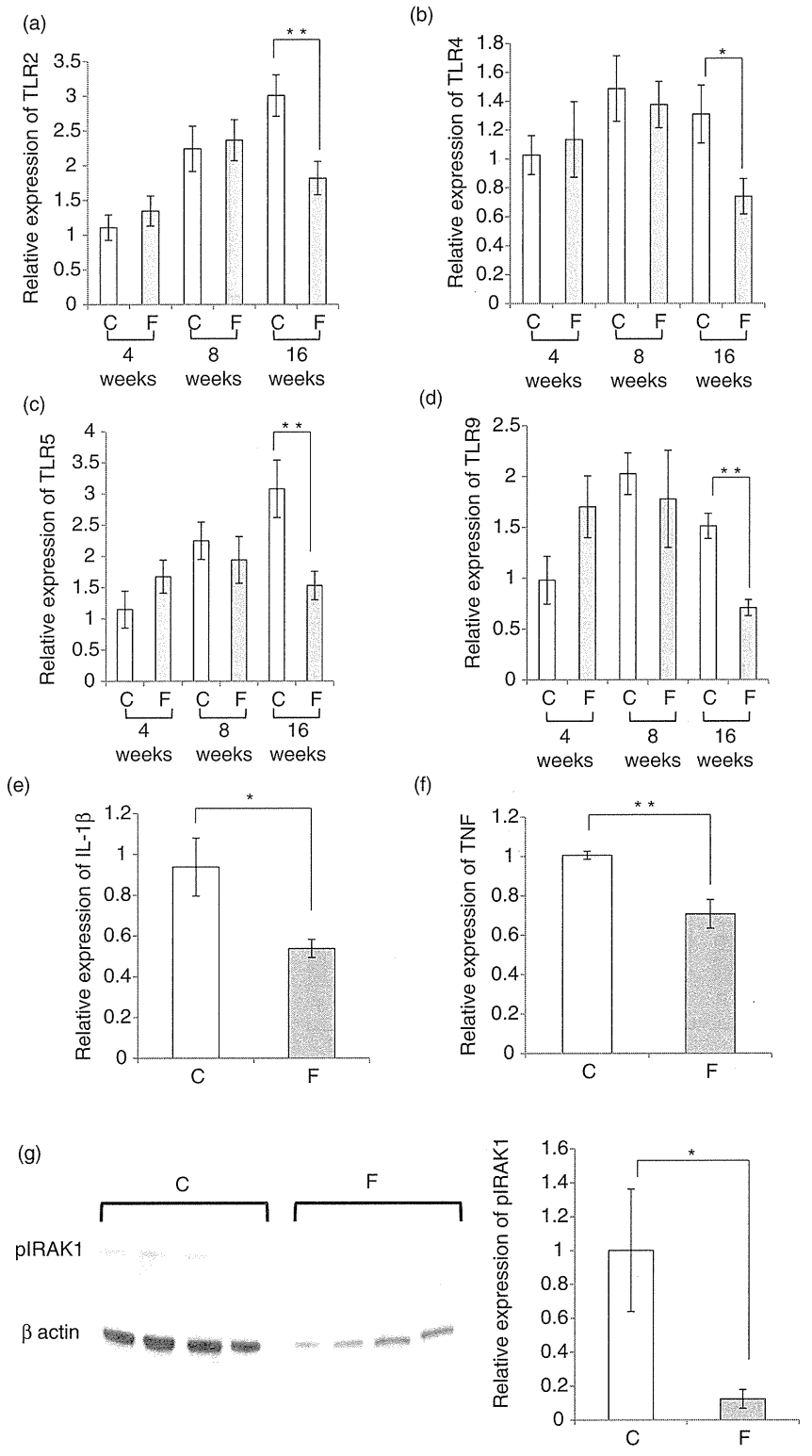

Figure 3 mRNA expression of inflammatory cytokines and Toll-like receptors in the small intestine of high fat diet (HFD)-fed and control mice. mRNA expression of TLR2 (a), TLR4 (b), TLR5 (c), and TLR9 (d) in the small intestine was significantly lower in HFD-fed mice (F) than in control mice (C) at 16 weeks. mRNA expression of IL-1β (e) and TNF (f) in the small intestine was also lower in group F than in group C at 16 weeks. Western blot analysis demonstrated a lower expression of phospho-interleukin-1 receptor-associated kinase1 (pIRAK) in the small intestine in group F than in group C at 16 weeks (g). (*$P < 0.05$, **$P < 0.01$).

pathways may induce immunotolerance, altered levels of microbiota, and bacterial overgrowth in the NAFLD small intestine. To investigate whether intestinal microbiota contribute to TLR expression, we eliminated them by treatment with non-absorbable broad-spectrum antibiotics.[24]

Body weight, serum ALT levels, and serum free fatty acids levels were significantly decreased in mice fed HFD and administered antibiotics (FA) compared with that in the mice fed HFD and water only (FC) (body weight: control diet and water only (CC), 28.9 g; control diet and antibiotics (CA), 28.6 g; FA, 34.7 g; FC, 51.9 g; serum ALT: CC, 19.5 IU/L; CA, 23.4 IU/L; FA, 34.7 IU/L; FC, 147.6 IU/L; serum free fatty acids: CC, 677.1 μEq/L; CA, 818.7 μEq/L; FA, 635.6 μEq/L; FC, 962.7 μEq/L; Fig. 4a–c). Histopathological findings from the livers of FC mice demonstrated the deposition of macronodular fat droplets in the centrilobular area and ballooning degeneration of hepatocytes. In contrast, FA mice showed a marked decrease in steatosis compared with the FC mice (Fig. 4d–g). The expression of TLRs (Fig. 5a–d) and inflammatory cytokines (Fig. 5e,f) was also significantly lower in the liver of FA mice than in that of FC mice. These data indicate associations among intestinal microbiota, TLR expression, and fatty acid metabolism.

Antibiotic treatment did not alter TLRs expression in the small intestine of HFD-fed mice

In the small intestine of mice fed the control diet, the expression of TLR2, TLR4, TLR5, and TLR9 was downregulated by antibiotic treatment (Fig. 6). However, contrary to expectations, the expression in HFD-fed mice did not alter (Fig. 6). These data suggest that microbiota contribute to TLRs expression in the small intestine of mice fed the control diet but not in that of mice fed HFD.

PA upregulated TLR2, TLR4, TLR5, and TLR9 expression in primary Kupffer cells

Because both serum free fatty acids and TLR expression were coincidentally suppressed in the intestinal bacterial eradication model, we examined whether fatty acids would alter TLR expression. First, we investigated TLR expression in primary Kupffer cells.

To determine the effects of fatty acids on TLR expression in Kupffer cells, PA was added to primary Kupffer cells for 24 h, where it induced the deposition of fat droplets (Fig. 7a,b). The mRNA expression of TLR2, TLR4, TLR5, and TLR9 was significantly higher in primary Kupffer cells treated with 10 μM PA for 24 h than in control cells (Fig. 7c).

Immunocytochemistry demonstrated that the expression of pIRAK1 was strongly positive in primary Kupffer cells with fat deposits (Fig. 7d). mRNA expression in IL-1β was not significantly different, but the expression of TNF was significantly higher in primary Kupffer cells exposed to 10 μM PA for 24 h than in controls (Fig. 7e,f). These findings indicate that PA may enhance the TLR signal pathway in Kupffer cells.

PA upregulated TLR4 and TLR9 expression in primary hepatocytes

Second, we examined TLR expression in primary hepatocytes treated with 100 μM PA for 24 h, which induced the deposition of fat droplets in these cells (Fig. 8a,b). mRNA expression of TLR4 and TLR9, but not that of TLR2 and TLR5 was significantly upregulated in primary hepatocytes treated with 100 μM PA for 24 h (Fig. 8c). The expression of IL-1β and TNF was significantly upregulated in primary hepatocytes treated with 100 μM PA for 24 h (Fig. 8d,e). These findings suggest that PA can, at least in part, enhance TLR signal pathways in hepatocytes.

DISCUSSION

MICE FED THE MCD diet demonstrated steatosis, macrophages accumulation, and clustering of neutrophils in the liver. Consequently, the expression of TLR4 and TNF-α was increased; however, the destruction of Kupffer cells prevented an increase in TLR4 expression,[10] indicating that increased expression levels had contributed to infiltration of inflammatory cells. It was reported that fatty liver in NASH resulted in increased liver injury and inflammation following intraperitoneal LPS injection in an MCD diet-induced NASH mouse model, suggesting that the MCD diet-induced NASH liver is sensitive to the TLR4 ligand LPS.[6] In our present model, mice fed HFD for 16 weeks developed steatosis with no histological evidence of inflammation and fibrosis, which is known as simple steatosis. However, the expression of inflammatory cytokines was upregulated, and our findings established that this was the mechanism by which TLR signal pathways were upregulated in the NAFLD liver prior to the development of steatohepatitis. Moreover, F4/80 staining revealed that this upregulation was not affected by an altered number of Kupffer cells but by changes in their activity in regard to inflammatory cytokine production. Our findings show that simple steatosis prior to NASH